NUCL SCI TECH (2018) 29:49
https://doi.org/10.1007/s41365-018-0391-3

Analysis of single-event transient sensitivity in fully depleted silicon-on-insulator MOSFETs

Jing-Yan Xu[1] · Shu-Ming Chen[1,2] · Rui-Qiang Song[1] · Zhen-Yu Wu[1] · Jian-Jun Chen[1]

Received: 12 July 2017 / Revised: 31 August 2017 / Accepted: 17 September 2017 / Published online: 13 March 2018

Abstract Based on 3D-TCAD simulations, single-event transient (SET) effects and charge collection mechanisms in fully depleted silicon-on-insulator (FDSOI) transistors are investigated. This work presents a comparison between 28-nm technology and 0.2-μm technology to analyze the impact of strike location on SET sensitivity in FDSOI devices. Simulation results show that the most SET-sensitive region in FDSOI transistors is the drain region near the gate. An in-depth analysis shows that the bipolar amplification effect in FDSOI devices is dependent on the strike locations. In addition, when the drain contact is moved toward the drain direction, the most sensitive region drifts toward the drain and collects more charge. This provides theoretical guidance for SET hardening.

Keywords Single-event transient · Charge collection · Bipolar amplification · Fully depleted silicon-on-insulator

This work was supported by the National Natural Science Foundation of China (Nos. 61434007 and 61376109).

✉ Jing-Yan Xu
jingyanxu@126.com

✉ Shu-Ming Chen
smchen_cs@163.com

1 College of Computer, National University of Defense Technology, Changsha 410073, China

2 National Laboratory for Parallel and Distributed Processing, National University of Defense Technology, Changsha 410073, China

1 Introduction

Fully depleted silicon-on-insulator (FDSOI) transistors are good candidates for use as technology scales down beyond the 28-nm node owing to short-channel-effect (SCE) suppression and low power consumption [1–3]. The radiation environment in space poses a major challenge to the reliability of electronic components in spacecraft. High-energy particles in space produce single-event effects (SEE) in transistors, which lead to multiple failures in the electronic systems [4]. It was proven that the FDSOI devices are more resilient to SEE than the bulk devices [5]. The FDSOI devices are also good candidates for applications in space.

Since the thin top silicon film reduces the charge-generation volume, FDSOI devices are considered to be able to mitigate single-event transient (SET) effects. [6] In recent years, many works have investigated the SET characteristics and charge collection mechanisms. However, while technology scales down beyond the 28-nm node, the parasitic bipolar amplification effect is further enhanced [7]. The power supply voltage is reduced and the charge stored in each sensitive node is reduced as well. These factors may increase the SET sensitivity of the FDSOI devices; therefore, the SET sensitivity and charge collection mechanisms in nanoscale FDSOI devices must be thoroughly understood. At present, research on charge collection mechanisms of FDSOI devices beyond the 28-nm node is still lacking. Previous studies have pointed out that the most sensitive region in the FDSOI devices is at the gate center [8–10]. However, a recent study proposed that the most sensitive region in the 22-nm FDSOI device is near the drain center [11, 12]. The mechanisms are not clear.

Thus, it is disadvantageous to find an effective hardening scheme.

In this paper, 3D-TCAD simulations are used to compare the most sensitive regions of the FDSOI devices between the 28-nm and 0.2-μm technology nodes. Simulation results indicate that the most SET-sensitive region in the FDSOI transistors is the drain region near the gate. The reason behind this is analyzed in detail from the standpoint of charge collection mechanisms. Furthermore, the effect of drain contact location on the most sensitive location and charge collection is investigated.

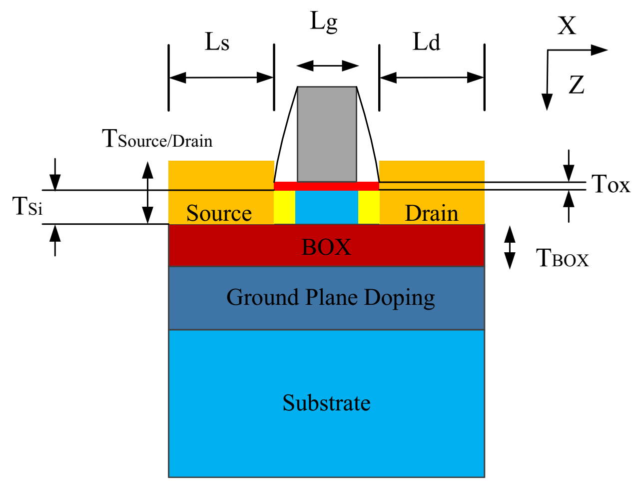

Fig. 1 (Color online) Schematic cross section of the 28-nm FDSOI device

2 Device structure and simulation setup

To simulate the SET in FDSOI devices, 3D-TCAD models are established. A 28-nm FDSOI negative channel metal oxide semiconductor (NMOS) is built and calibrated according to the ST28 FDSOI PDK. The high-*K* dielectric layer and metal gate technology is used. Figure 1 shows a cross-sectional schematic diagram of the 28-nm FDSOI device. Figure 2 shows the *I*–*V* characteristic curves. The 0.2-μm FDSOI NMOS is built and calibrated using published data [13]. Figure 3 shows the *I*–*V* characteristic curves of the 0.2-μm FDSOI device. The design parameters are listed in Table 1.

The n-type devices are biased in the off-state during the TCAD simulations. The drain is biased at the supply voltage V_{dd}, while the source, gate and ground planes (GP) contacts are grounded. The power supply voltages of the 28-nm devices and 0.2-μm devices are 1 and 1.8 V, respectively. The total simulation time is T_s = 300 ps and the heavy ions start showing impacts at T_i = 100 ps. All

Fig. 2 (Color online) *I*–*V* characteristic curves of the 28-nm FDSOI device **a** I_d–V_g curves, and **b** I_d–V_d curves

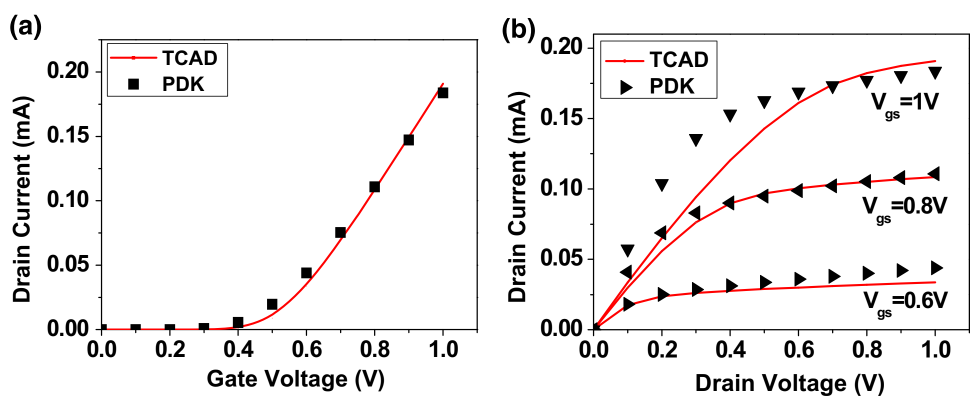

Fig. 3 (Color online) *I*–*V* characteristic curves of the 0.2-μm FDSOI device **a** I_d–V_g curves, and **b** I_d–V_d curves

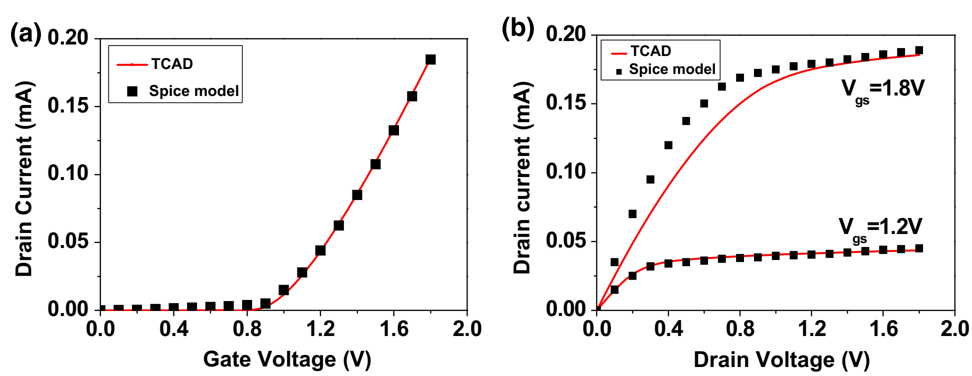

simulations are conducted for the normal incidence. The heavy ions strike the devices at various locations from source to drain, and the collected charge is given by the drain current integration over the transient duration. The collected charge by drift–diffusion (DD) is simulated using the device with the floating source.

Table 1 FDSOI physical parameters

Parameters	28 nm	0.2 µm
L_g (nm)	30	200
L_d (nm)	120	690
W (nm)	210	1000
T_{OX} (nm)	0.5	5
T_{Si} (nm)	7	50
T_{BOX} (nm)	25	100
W_{spacer} (nm)	10	100
$T_{source/drain}$ (nm)	17	50
Φ_M(eV)	4.65	–

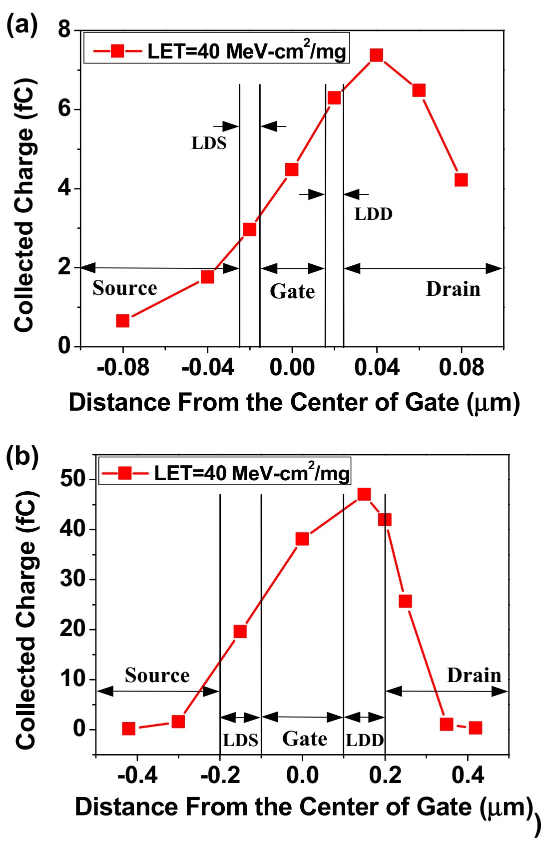

Fig. 4 (Color online) Collected charge versus strike location: **a** 28-nm device, and **b** 0.2-µm device

3 Simulation results

The strike location is from the source center to the drain center. The collected charge is shown in Fig. 4. The source is in the negative direction and the drain is in the positive direction. As shown in Fig. 4, the most sensitive region of the 28-nm FDSOI devices is the drain region at 0.04 µm from the gate center, and the most sensitive region of the 0.2-µm FDSOI devices is the drain region at 0.15 µm from

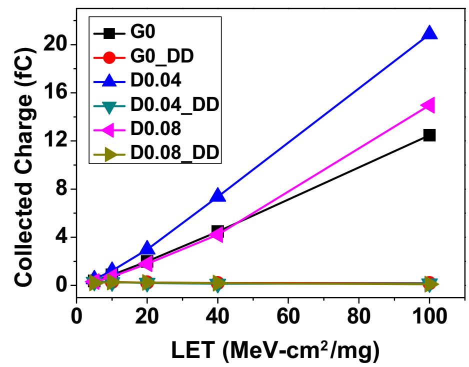

Fig. 5 (Color online) Collected charge versus LET in a 28-nm FDSOI device

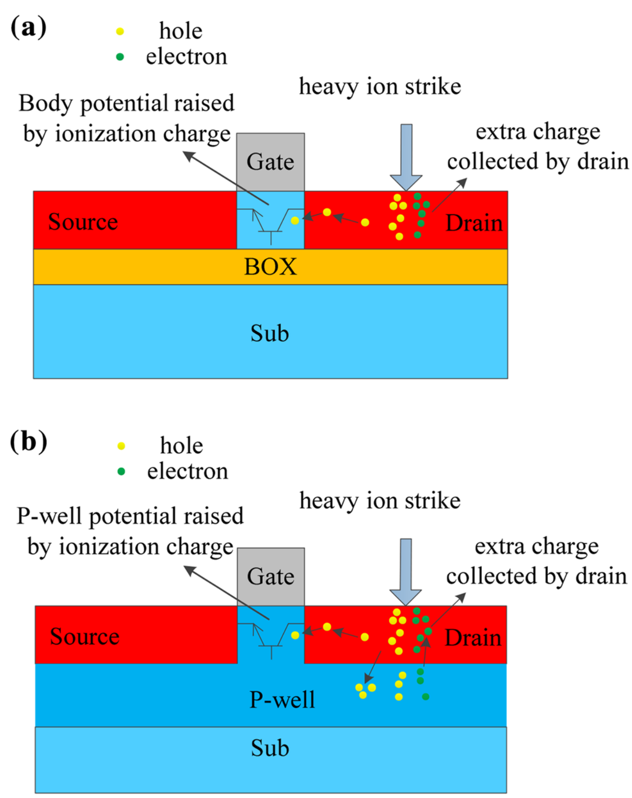

Fig. 6 (Color online) Charge collection mechanisms in **a** an FDSOI device, and **b** a Si-bulk device

the gate center. The drain region near the gate is the most sensitive. The SET sensitivity in the center of the gate and the drain is similar under the 28-nm process. However, the drain center is not sensitive under the 0.2-μm process. This is consistent with the previous simulation results. The reason is analyzed in detail from the standpoint of charge collection mechanisms in the next section.

For brevity, in this paper, the gate center is denoted as G0 and the drain region at *x*-μm from the gate center is denoted as *Dx*. Whereas the strike locations are G0, D0.04 and D0.08, the collected charge in the 28-nm FDSOI devices versus the linear energy transfer (LET) relationship is given in Fig. 5. The latter also shows that the charge was collected by drift–diffusion (DD). We observed that the collected charge increases with the LET depending on the bipolar amplification effect. In contrast, the charge collected by drift–diffusion is saturated. In addition, the bipolar amplification effect is affected by the strike location.

4 Discussion

Many studies have reported on the heavy-ion-induced charge collection mechanisms in CMOS transistors [14–17]. It has been shown that the charge collection process consists of drift–diffusion and the parasitic bipolar amplification. Owing to the isolation of the buried layer, the charge-generation volume in FDSOI devices is very small. Thus, the charge collected by drift–diffusion is very limited, especially in the FDSOI device beyond the 28-nm process node. However, owing to the ultrathin body, the body potential is easily varied and raised by the ionization charge, which triggers the parasitic bipolar junction transistor (BJT). Thus, a large number of electrons are injected from the source into the drain. The simulation results shown in Fig. 5 also confirm that the parasitic bipolar amplification is dominant in the charge collection.

In addition, the body potential raised by the ionization charge is related to the strike location, and the recovery rate is also different. Therefore, the bipolar amplification effect is dependent on the strike location. It is the decisive factor for the location of the sensitive region.

Compared to the gate center, when the heavy ions are incident on the drain region, the ionized electrons can be collected more quickly. Subsequently, a large number of holes are left and moved to the body region through drift–diffusion to raise the body potential. The bipolar amplification is triggered quickly. However, as shown in Fig. 6, when the strike location is too far away from the body, the situation is different. Unlike the holes in the bulk silicon

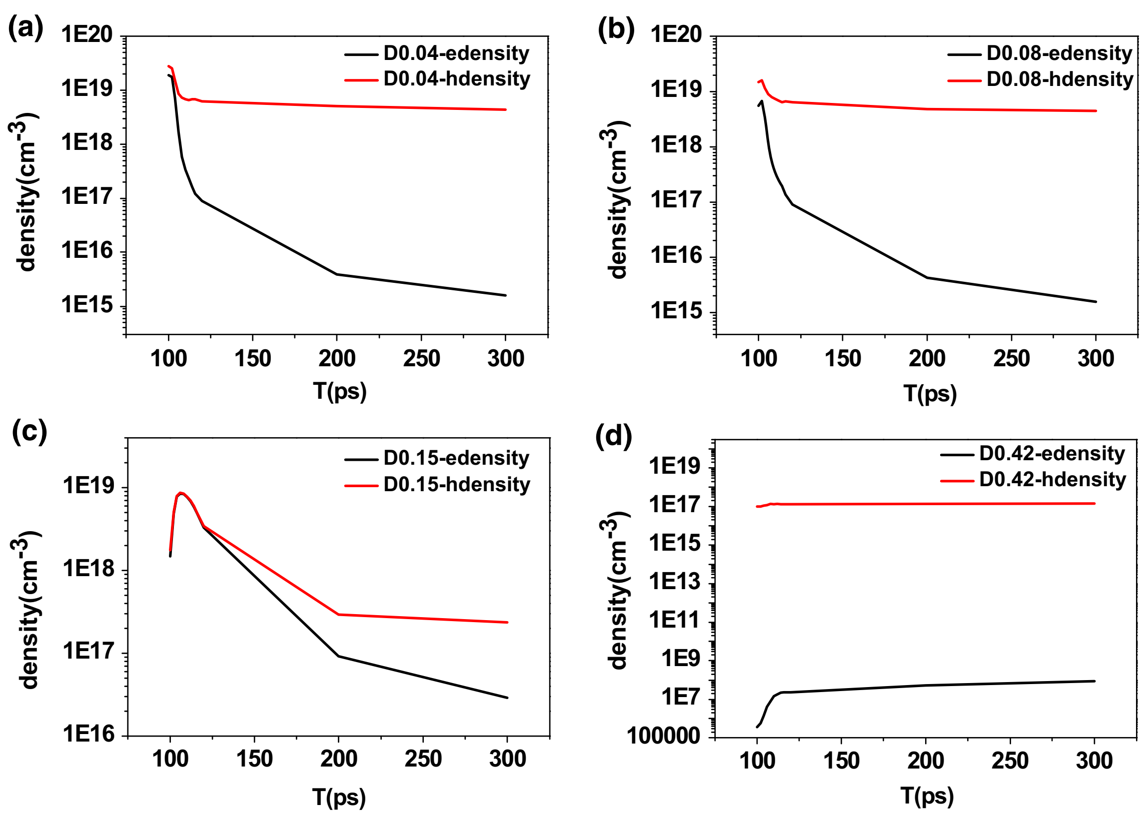

Fig. 7 (Color online) Electron and hole density variation in the body region after heavy-ion injection with different strike locations at an LET of 40 MeV-cm^2/mg **a**, **b** in a 28-nm device, and **c**, **d** in a 0.2-μm device

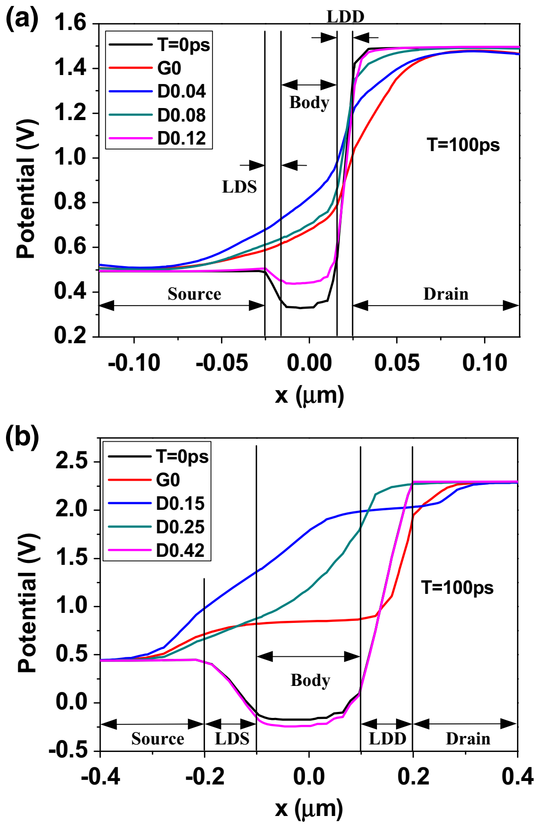

Fig. 8 (Color online) Potential distribution in **a** a 28-nm device, and **b** a 0.2-μm device

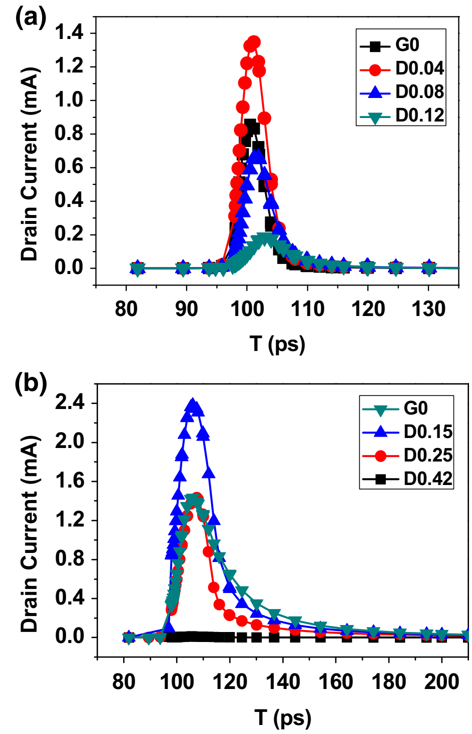

Fig. 9 (Color online) The SET current in **a** a 28-nm device, and **b** a 0.2-μm device; LET = 40 MeV-cm^2/mg

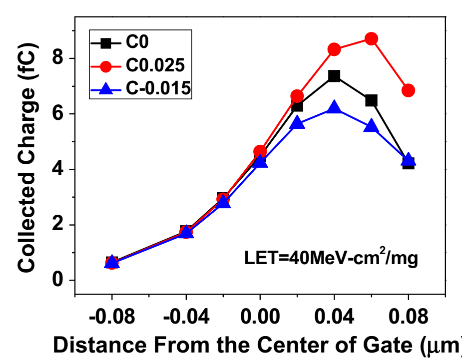

Fig. 10 (Color online) Collected charge versus strike location with various contact locations

device that move to the p-well below the drain to raise the p-well potential, the holes in the FDSOI device must pass through the long doping drain region to reach the body. In particular, in the heavily doped region, recombination is enhanced and mobility is degraded [18]. Therefore, it is difficult for the holes to reach the body. As shown in Fig. 7d, the center of the drain (D0.42) in a 0.2-μm FDSOI device is not sensitive because it is too far from the body for enough holes to reach the body to trigger bipolar amplification. In contrast, as shown in Fig. 7b, the center of the drain (D0.08) in a 28-nm FDSOI device is sensitive because it is closer to the body. The most sensitive region in the FDSOI devices must meet two conditions. One condition is that the ionized electrons can be quickly collected. The other condition is that the holes can simultaneously reach the body quickly. As shown in Fig. 7a, c, the drain region near the gate is most sensitive owing to the balance of the two conditions.

Figure 8 shows the potential distribution along the channel length direction at $T = 100$ ps and LET = 40 MeV-cm^2/mg. Figure 9 shows the SET current. When the strike location moves from the gate center (G0) to the drain (*Dx*), the body potential and the SET current are first raised and then lowered in both the 28-nm and 0.2-μm devices. The bipolar amplification effect is enhanced when the body potential is raised. This coincides with the variety in charge collection when the strike location moves from the gate center to the drain, as shown in Fig. 4. This proved that the bipolar amplification effect is the decisive factor in the charge collection in FDSOI devices.

Simultaneously, as shown in Fig. 8a, in the 28-nm device, when the heavy ion is incident on the gate center (G0) or on the drain center (D0.08), the body potential is similar. Therefore, as shown in Figs. 4a and 9a, the SET sensitivity on the drain center and the gate center in a 28-nm device is similar. However, as shown in Fig. 8b, when the heavy ion is incident on the drain center (D0.42) in the 0.2-μm device, the body potential is almost unchanged from that before the incident. Therefore, as shown in Figs. 4b and 9b, the drain center is not completely sensitive. This phenomenon is consistent with the analysis above. The drain center is so far from the body that not enough holes can reach the body to raise the body potential and trigger the bipolar amplification in the 0.2-μm device.

In addition, the drain contact location is related to the location of the most sensitive region and the charge collection. As shown in Fig. 10, the contact at the drain center is denoted as C0, and the contact at x-μm from the drain center is denoted as Cx. The source is in the negative direction, and the drain is in the positive direction. When the drain contact is moved toward the drain direction, the most sensitive region drifts toward the drain and collects more charge. The ionized electrons in the drain can be quickly collected in this case, as discussed above.

5 Conclusion

The SET sensitivity and charge collection are strike-location sensitive because the bipolar amplification effect is affected dramatically by the strike location. The most sensitive region in n-type FDSOI devices must meet two conditions. One condition is that the ionized electrons can be quickly collected. The other condition is that the holes can simultaneously reach the body quickly. The most SET-sensitive region in the FDSOI devices is the drain region near the gate, owing to the balance of the two conditions. When the drain contact is moved toward the drain direction, the most sensitive region drifts toward the drain and collects more charges. As the semiconductor technology scales down further, the drain will be more sensitive than the gate. This work provides some helpful guidance on suppressing the bipolar amplification effect to mitigate the SET sensitivity in FDSOI devices.

References

1. E. Simoen, M. Gaillardin, P. Paillet et al., Radiation effects in advanced multiple gate and silicon-on-insulator transistors. IEEE Trans. Nucl. Sci. **60**, 1970 (2013). https://doi.org/10.1109/TNS.2013.2255313
2. S. Chouksey, J.G. Fossum, S. Agrawal, Insights on design and scalability of Thin-BOX FD/SOI CMOS. IEEE Trans. Electron Devices **57**, 2073 (2010). https://doi.org/10.1109/TED.2010.2052420
3. S. Luan, H. Liu, R. Jia et al., 2-D analytical modeling of dual material gate fully depleted SOI MOSFET with high-k dielectric. Acta Phys. Sin. **57**, 3807 (2008). **(in Chinese)**
4. P.E. Dodd, M.R. Shaneyfelt, J.R. Schwank et al., Current and future challenges in radiation effects on CMOS electronics. IEEE Trans. Nucl. Sci. **57**, 1747 (2010). https://doi.org/10.1109/TNS.2010.2042613
5. O. Musseau, Single-event effects in SOI technologies and devices. IEEE Trans. Nucl. Sci. **43**, 603 (1996). https://doi.org/10.1109/23.490904
6. L. W. Massengill, B. L. Bhuva, W. T. Holman et al., Technology scaling and soft error reliability. in *Proceedings of IEEE International Reliability Physics Symposium,* 2012, p. 3C-1. https://doi.org/10.1109/irps.2012.6241810
7. K. Castellani-Coulié, D. Munteanu, J.L. Autran et al., Simulation analysis of the bipolar amplification induced by heavy-ion irradiation in double-gate MOSFETs. IEEE Trans. Nucl. Sci. **52**, 2137 (2005). https://doi.org/10.1109/TNS.2005.860680
8. K. Hirose, H. Saito, Y. Kuroda et al., SEU resistance in advanced SOI-SRAMs fabricated by commercial technology using a rad-hard circuit design. IEEE Trans. Nucl. Sci. **49**, 2965 (2002). https://doi.org/10.1109/TNS.2002.805978
9. M.J. Gadlage, P. Gouker, B.L. Bhuva et al., Heavy-ion-induced digital single event transients in a 180 nm fully depleted SOI process. IEEE Trans. Nucl. Sci. **56**, 3483 (2009). https://doi.org/10.1109/TNS.2009.2033688
10. D. Tang, Y. Li, G. Zhang et al., Single event upset sensitivity of 45 nm FDSOI and SOI FinFET SRAM. Sci China Tech. Sci. **56**, 780 (2013). https://doi.org/10.1007/s11431-012-5125-x
11. J. Bi, R.A. Reed, R.D. Schrimpf et al., Neutron-induced single-event-transient effects in ultrathin-body fully-depleted silicon-on-insulator MOSFETs. in *Proceedings of IEEE International Reliability Physics Symposium,* 2013, p. SE-2. https://doi.org/10.1109/irps.2013.6532109
12. J. Bi, G. Liu, J. Luo et al., Numerical simulation of single-event-transient effects on ultra-thin-body fully-depleted silicon-on-insulator transistor based on 22 nm process node. Acta Phys. Sin. **62**, 208501 (2013). https://doi.org/10.7498/aps.62.208501. **(in Chinese)**
13. J. Bi, B. Li, Z. Han et al., 3D TCAD simulation of single-event-effect in n-channel transistor based on deep sub-micron fully-depleted silicon-on-insulator technology. in *Proceedings IEEE International Conference on Solid-State and Integrated Circuit Technology*. Oct. 28–31, 2014, Guilin, China, p.1. https://doi.org/10.1109/icsict.2014.7021288
14. V. Ferlet-Cavrois, L.W. Massengill, P. Gouker, Single event transients in digital CMOS—a review. IEEE Trans. Nucl. Sci. **60**, 1767 (2013). https://doi.org/10.1109/TNS.2013.2255624
15. P. Huang, S. Chen, J. Chen, Mechanism of floating body effect mitigation via cutting off source injection in a fully-depleted silicon-on-insulator technology. Chin. Phys. B **25**, 036103 (2016). https://doi.org/10.1088/1674-1056/25/3/036103
16. Z. Liu, S. Chen, J. Chen et al., Parasitic bipolar amplification in single event transient and its temperature dependence. Chin. Phys. B **21**, 099401 (2012). https://doi.org/10.1088/1674-1056/21/9/099401
17. J. Chen, S. Chen, B. Liang et al., New insight into the parasitic bipolar amplification effect in single event transient production. Chin. Phys. B **21**, 016103 (2012). https://doi.org/10.1088/1674-1056/21/1/016103
18. D. Neamen, *Semiconductor physics and devices* (McGraw-Hill, New York, 2002), p. 157